A New Model of Human Steering Using Far-Point Error Perception and Multiplicative Control

Conference Paper · October 2018

DOI: 10.1109/SMC.2018.00218

2 authors:

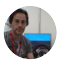
Miguel Martínez-García
Loughborough University


Timothy Gordon
University of Lincoln

A New Model of Human Steering using Far-point Error Perception and Multiplicative Control

Miguel Martínez-García, Timothy Gordon
School of Engineering
University of Lincoln
Brayford Pool, LN6 7TS, UK
Email: {mmartinez, tgordon}@lincoln.ac.uk

***Abstract*—In this paper, a new steering control model is introduced, motivated by several characteristics of human driving. The model uses as input an *optical variable* portraying visual information directly accessible to the driver: the *splay error*, representing the lane positioning aspect of driving. The splay error is regulated through a multiplicative control model; this approach displays similar statistical properties to those found in human compensatory control. Further, multiplicative control exhibits steering pulse behavior related to human steering. A second input variable in the model, the *critical normalized yaw rate*, reflects the information from the far region of the road. The parameters of the model are optimized for low and high vehicle speeds through a genetic algorithm. With the fitted parameters, the response of the model is compared to driver behavior by means of steering workload measurement, and validated with naturalistic driving data.**

I. Introduction

Human driving, and especially human steering control, involves significant complexity from the perspective of signal processing. On the other hand, human manual control can be understood via simple models. Until now such simple models do not represent the detailed actions of the human driver, and it is the aim of this paper to develop further the scientific understanding of human control behavior in driving using elementary control models.

A good deal of the complexity in driver behavior is produced at the visual acquisition stage, and a range of concepts regarding eye target acquisition populate the literature, from the stochastic nature of the eye motion [1], [2], to variable timing of target recognition [3], [4].

Nevertheless, many human steering control models employ standard engineering variables to serve as visual input. In some models, these variables represent lateral offsets and their respective derivatives. For example, the classical driver model by Kondo uses a prediction of the lateral offset after a fixed preview time [5]. Similarly, in [6] an optimal control model is proposed which acts as a minimizer of an integrator of the predicted lateral deviation. This approach always comes with one caveat: different visual effects, such as *size constancy*, imply that human's central nervous system (CNS) may generate significant errors when estimating lateral distance [3]. Equivalently, it is easier to design computer vision systems that estimate angles than distances, as angular information can be easily inferred from the projection of images over a two-dimensional subspace.

In this paper a new model of steering control, based on visual inputs consistent with actual driver behavior, is designed. As drivers are known to use both, the near and the far field information of the road [2], two variables are used: the *splay error* – which captures the near field aspect of driving – and the *critical normalized yaw rate* (CNYR) [7] – which reflects the far region information of the visual field. The splay error is an *optical variable*, as it is directly perceived by the projection of the road markings on the retina.

Regarding the control law that responds to the input variables, previous research has shown that the control responses of human subjects, in compensatory and pursuit tracking tasks, can be characterized by a multiplicative controller [8]. This results from evidence that the magnitude of human's motor control pulses is well approximated by a log-normal probability distribution. Hence, to respond to the near field information at low speeds a *multiplicative human control* (MHC) scheme is employed in the presented model. For the far field visual information, which is more related to driving at higher speeds, integral control is utilized over the CNYR, since this variable has been demonstrated to be correlated to the steering signal in naturalistic driving data (NDD) at $\approx 30\,\mathrm{ms}^{-1}$ [7]. Additionally, an open-loop component is added to the model to compensate for the curvature of the road with a minimal delay.

The parameters of the proposed model are first fitted through a genetic algorithm. Then, the model is contrasted to another modeling approach, that of pulse control models [7], [9]. Further, the behavior of the model is compared and validated with that of human drivers. This is done through a metric to assess driver's alertness, the *steering entropy* [10], and NDD.

The presented model is *biofidelic*, as it is based on knowledge originated from analyzing actual human control response. Its proposed applications are shared-control algorithms, ground vehicle testing and the design of autonomous and semi-autonomous driving systems for ground vehicles, such as the relevant topic of obstacle avoidance systems [11].

II. Visual Input Variables in Driver Behavior

It is known, since the influential experiments by Hubel and Wiesel, that the CNS is specially well adapted to detect and interpret angular misalignments. Hubel and Wiesel performed a series of experiments, by recording neuron firings in a cat's brain, that showed the existence of a corresponding array of

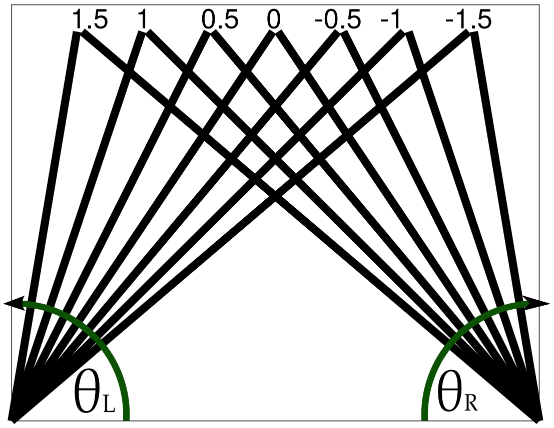

Fig. 1: Splay angles (θ_L and θ_R) in a hypothetical road scene for different lateral offsets, from $-1.5\,\mathrm{m}$ (vehicle displaced to the right) to $1.5\,\mathrm{m}$ (to the left).

columns of neurons in the primary visual cortex. These columns are arranged in perpendicular alignment to the pial surface and, visually perceived lines oriented or moving along different angles, excite different columns in an orderly manner [12]. A recent study has showed that human's primary visual cortex is also organized in orientation columns [13]. Thus angular perception is directly mapped to the primary visual cortex, the part of the brain that first processes visually acquired inputs.

Consequently, borders and edges are very important in visual perception [3]. This has its importance for driving; driving a vehicle is a *boundary departure avoidance* task, and not necessarily an offset minimization task. Along these lines, here it is assumed that human drivers respond primarily to angular information for lane keeping.

There exist driver models in the literature that use angular variables as input. For example in [14] it is described a model, essentially a PI controller, which is based on visually interpreted angles to a near and a far point. Even here the angles are assumed to be estimated in inertial coordinates, and not directly perceived from the forward road scene.

A. Splay angles and splay error

The retina in the human eye, which is where the photoreceptors are located, is fundamentally a two dimensional surface. Thus vision can be regarded as a projection from a three-dimensional space to a two-dimensional space [3]. The low-speed model presented here employs only visual information which is directly projected into the retina; by considering the projection of the left and right markings of a traffic lane over a flat surface, two angles are delineated: θ_L and θ_R (Fig. 1). These angles are referred to as *splay angles*, and are defined as the interior angles of the projections. The potential importance of the splay angles in course control has already been mentioned in the literature [15], [16].

The splay angles are easily accessible for the human driver as well as for computer vision systems. Thus, in this paper it is considered that human lane keeping at low speeds is a response to the difference between the splay angles. That is, the human driver is assumed to employ as control variable the *splay error* (Θ):

$$\Theta = \theta_R - \theta_L. \tag{1}$$

The splay error has only meaning in the near distance with respect to the position of the vehicle, as in the far distance its projection is altered by the road geometry when the road is not straight. Nevertheless, because in non-curved roads Θ can be inferred by looking far ahead in the road too, it is a variable robust to saccadic motions. Indeed, it is known that drivers rarely gaze at the near region of the road [1], although this does not imply that they do not perceive it through peripheral vision; the road positioning capabilities of drivers are reduced when the near region of the road is occluded [2].

B. Critical normalized yaw rate (CNYR)

Usually in human driver modeling it is regarded that drivers use both, the near and the far information of the road [14]. Drivers consistently look ahead from $1\,\mathrm{s}$ to $2\,\mathrm{s}$ into the future [1], [2]. Taking this into account, the CNYR is here considered to serve as far-point input variable to the model.

The CNYR is representative of human driver behavior, as it displays higher correlation with steering pulses in NDD than other lane keeping metrics – such as the near and far angles in [14] – at relatively high speeds ($\approx 30\,\mathrm{ms}^{-1}$) [8].

The *critical yaw rate* is the yaw rate ($\dot{\psi}$) that if sustained would cause the vehicle exiting the driving lane at a distance d [17]. It is expressed independently for each road boundary. For the left boundary it is given by the following relation:

$$\dot{\psi}^{\mathrm{L}}_{\text{crit}} = \frac{2U \sin \phi_{\mathrm{L}}}{d_{\mathrm{L}}}, \tag{2}$$

where U is the velocity of the vehicle and d_L the distance from the left front tire to a predefined boundary point in the left boundary. ϕ_L is the left azimuth angle – i.e., the heading-relative bearing to the left boundary point. The right critical yaw rate ($\dot{\psi}^{\mathrm{R}}_{\text{crit}}$) is equivalently defined.

From the critical yaw rate the CNYR (χ) results:

$$\chi = \frac{\dot{\psi} - 1/2\left(\dot{\psi}^{L}_{\text{crit}} + \dot{\psi}^{R}_{\text{crit}}\right)}{1/2\left(\dot{\psi}^{L}_{\text{crit}} - \dot{\psi}^{R}_{\text{crit}}\right)}. \tag{3}$$

The CNYR is a non-dimensional variable combining the information of both critical yaw rates – left and right. When $\dot{\psi} = \dot{\psi}^{\mathrm{L}}_{\text{crit}}$ or $\dot{\psi}^{\mathrm{R}}_{\text{crit}}$ then $\chi = 1$ or -1 respectively. It suffices to maintain $|\chi| < 1$ in order to keep the vehicle within the lane boundaries at all times.

III. Low Speed Driver Model

A. A multiplicative model of human control

Statistical analysis of steering angle signals, recorded from human subjects performing compensatory and pursuit tracking tasks, shows that the probability distribution of the magnitude of the steering response is well approximated by a log-normal probability distribution [8] (Fig. 2).

In addition, it can be verified that the log-normal distribution arises as a result of a multiplicative process; for a multiplicative process of the form

$$G_{t_k} = \xi_{t_k} G_{t_{k-1}} = G_{t_0} \prod_{i=t_1}^{t_k} \xi_i, \tag{4}$$

where $(t_i, t_{i+1}) \subset \mathbb{R}^+ \cup \{0\}$ are equispaced time intervals and $G_{t_0} > 0$, $\xi_i > 0$, one can take logarithms resulting in

$$\log G_{t_k} = \log G_{t_0} + \sum_{i=t_1}^{t_k} \log \xi_i. \tag{5}$$

Now, if ξ_i are identically distributed and independent random variables, the *central limit theorem* can be applied to the summation term of (5). This means that for large values of k, $\log G_{t_k}$ will approximately follow a normal probability distribution. Therefore, G_{t_k} will approximately follow a log-normal distribution. From these considerations, a multiplicative human-control (MHC) model was proposed in [8].

By analogy with (4), the MHC approach is as follows; considering discrete time steps t_k for $k = 1, 2, \dots, f$, the steering control response of the model ($C_M(t_k)$) at time t_k to an error e_{t_k} is determined by the relations:

$$C_M(t_k) \equiv K_M S_{t_k} M_{t_k} \tag{6a}$$

$$M_{t_k} \equiv L^{n_\tau} \left\{ \left| \frac{e_{t_k}}{e_{t_{k-1}}} \right|^\rho \right\} M_{t_{k-1}} \tag{6b}$$

$$S_{t_k} \equiv \operatorname{sgn}\left(L^{n_\tau} \{ e_{t_k} \} \right), \tag{6c}$$

where K_M is the controller gain. The direction of the control action is determined by the sign function S_{t_k}, which applies the lag operator L^{n_τ} to the perceived error (e_{t_k}) at time t_k by n_τ time steps – that is, there is a delay in the response of $\tau = n_\tau (t_k - t_{k-1}) \coloneqq n_\tau \Delta_t$ seconds. The magnitude of the multiplicative response before applying the gain (M_{t_k}), is the result of applying the multiplicative rule over the ratio of errors at two consecutive time steps. Over this ratio an exponent $\rho > 0$ is applied, after delaying its value – again by τ seconds. The parameter ρ regulates how quick the model adapts its response when the error varies.

The right hand side of (6b) can be interpreted as a multiplicative derivative [18]:

$$f^*(t) = \lim_{\Delta_t \to 0} \left\{ \frac{f(t + \Delta_t)}{f(t)} \right\}^{\frac{1}{\Delta_t}} \tag{7}$$

The MHC model was validated with steering angle signals recorded from human subjects in [8].

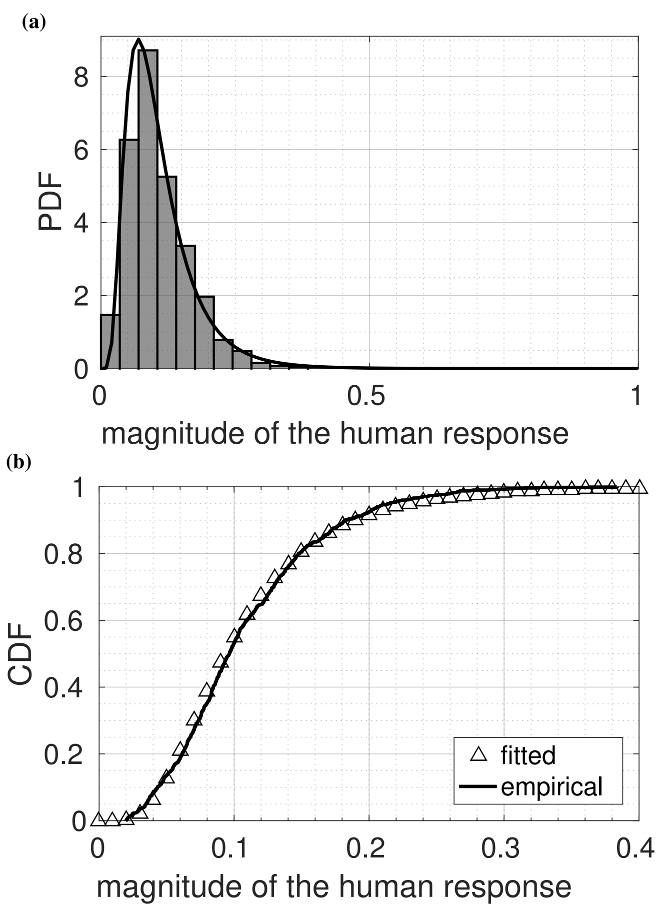

Fig. 2: (a) Normalized histogram for the responses of ten human subjects combined – from a steering wheel angle sensor – along with the fitted log-normal probability density function [8]. (b) Fitted cumulative density function and empirical values.

B. Multiplicative steering control for low-speed driving

For low-speed driving, local compensatory feedback is expected to dominate the steering angle signal. The MHC is here implemented for low-speed driving. The input error to the MHC model is taken to be the splay error – $e_{t_k} = \Theta(t_k)$, and the output the *steering wheel angle* (SWA) – $C_M(t_k) = \delta(t_k)$.

Typically, the human operator is assumed to be a discrete actuator with a cycle time of $\approx 50\,\mathrm{ms}$ [14], and with response delays that are in the range $133 - 528\,\mathrm{ms}$ [19]. Thus the Δ_t and τ are set to $50\,\mathrm{ms}$ and $250\,\mathrm{ms}$ ($n_\tau = 5$) respectively.

Additionally, humans present thresholds in visual perception. These are established by the CNS to filter potential residual firing occurring within the photoreceptors [3]. In consequence, a threshold is set in the MHC model so that it responds only when $|\Theta(t_k)| > 1\,\mathrm{deg}$.

With these settings, the parameters in the MHC scheme were fitted using multiobjective optimization through a genetic algorithm. The algorithm run a simulation in the IPG Carmaker environment [20] at $6\,\mathrm{ms}^{-1}$ in a straight road. A random torque perturbation over the heading of the vehicle was added every $0.1\,\mathrm{s}$. The two dimensional cost function consisted on the *total splay error* (T_Θ) and the *steering workload* (W_s) [21]:

$$T_\Theta = \int_0^T \Theta^2(t)\, dt \tag{8a}$$

$$W_s = \int_0^T \dot{\delta}^2(t)\, dt. \tag{8b}$$

The optimization process yielded optima near $K_M \approx 1.11$ and $\rho \approx 0.13$. Figure 3 displays the steering response $\delta(t_k)$

of the MHC model with the fitted parameters, along with the splay error $\Theta(t_k)$. The MHC model produces *ballistic movements* in the response. This is supportive of the MHC model to behave in a biofidelic manner – i.e., to approximately reproduce the principles of human control – as the hypothesis of human control consisting in ballistic movements has long been recognized [22], [23]. The same concept was further investigated in [24], where it was acknowledged that motor movements are a superposition of different motor primitives. More specifically, and with respect to steering control, steering signals have been decomposed into bell shaped steering pulses [25], and by using an unsupervised learning method, elementary steering pulses were extracted from NDD in [7].

Steering control laws that mimic the ballistic behavior exhibited by humans have already been proposed [7], [9]. It is relevant though, that the MHC model generates ballistic behavior without that being *a priori* considered during the design of the controller.

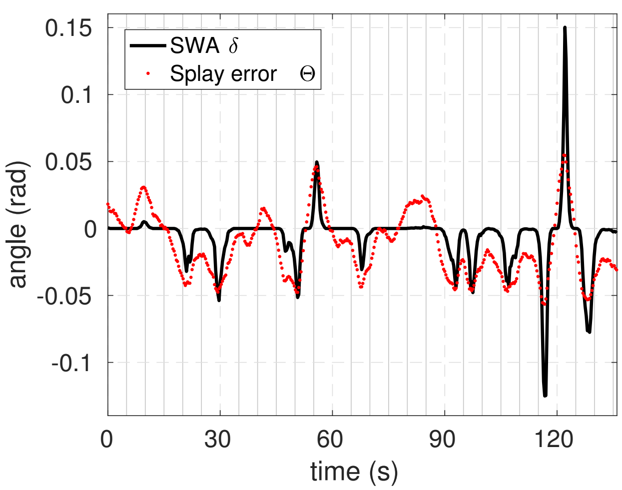

Fig. 3: Splay error (Θ) and SWA (δ) for a simulation of a Toyota Camry 2006 running with the control parameters $K_M = 1.11$ and $\rho = 0.13$ in a straight lane at $6\,\mathrm{ms}^{-1}$.

IV. Human-centered Driver Model

A. Far-point error for steering control

At higher speeds, the steering response of the model (6) becomes excessively jerky when only the splay error is available. The same effect is observed in humans when only the near region of the road is accessible [2]. This is caused by the lack of preview information to compensate for the response delay τ. Thus far-point preview control needs to be incorporated into the model. Here, integral control results in a steering-rate proportional to the CNYR and with the same response delay τ:

$$\frac{dC_\chi(t)}{dt} = -K_\chi L^{n_\tau}\{\chi(t)\}. \tag{9}$$

The preview distance to the left and right boundary points ($d_{L,R}$) is set at a preview time of $T_p = 1.5\,\mathrm{s}$ according to the current speed of the vehicle ($d_{L,R} = UT_p$).

Besides error corrective control, human drivers use *guidance level control* to anticipate changes in the road geometry [15]; driving is a combination of feed-forward and feedback actions [7], [15]. According to the relation for the Ackermann angle, the feed-forward component of driving is reflected in the model by the relation:

$$C_\kappa(t_k) = r_s\kappa(t_k)L \tag{10}$$

where r_s is the steering ratio, κ the road curvature and L the wheelbase of the vehicle. Because drivers do anticipate changes in road curvature, there is no response delay in this term. The curvature of the road can be estimated by looking at the *tangent point* of the road [2].

Hence, from the superposition of the three control terms in (6a), (9) and (10), the proposed model results (Fig. 4):

$$\delta(t_k) = C_M(t_k) + C_\chi(t_k) + C_\kappa(t_k). \tag{11}$$

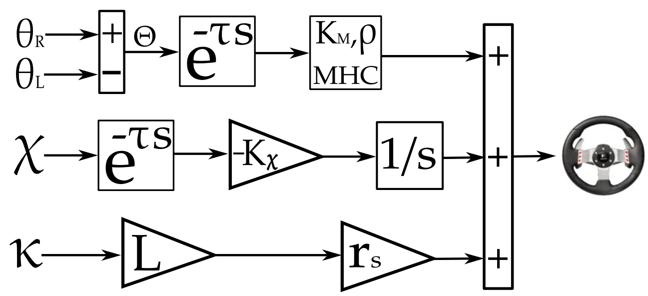

Fig. 4: Schematic of the proposed steering control model. The first two terms (C_M and C_χ) act as error compensators after a delay time τ, while the last term is a feed-forward controller. Only the last two terms (C_χ and C_κ) include road preview.

B. Model parameters optimization at high speed

The parameters of model (11) were fitted with the same setup as in Section III-B, with the exceptions that the ground vehicle simulation run over an oval circuit with curves of $200\,\mathrm{m}$ radius and at a speed of $30\,\mathrm{ms}^{-1}$. The resulting optima in the Pareto front were found to be clustered around the values $K_M \in [1.3, 2.3]$, $\rho \in [0.018, 0.027]$ and $K_\chi \in [0.24, 0.31]$ (Fig. 5). With the chosen cost function (8), the effect of the multiplicative controller becomes negligible ($\rho \approx 0$) at high speeds. However, there is no reason to believe that human steering control corresponds to minimizing the splay error (8b) and the steering workload (8b), but rather to act as a *satisficing controller*. Therefore, steering workload analysis and parameter estimation through NDD is performed to make the response of the model correlate more closely to that of human drivers.

C. Driver workload analysis and Model Validation with NDD

To compare the behavior of the model with that of human drivers, analysis of the steering signal through the *steering entropy* metric (described in the Appendix) is conducted. Different values of steering entropy (H_p) reflect different levels of driver attention directed to the steering task. For example, $H_p = 0.47$ approximately matches the steering entropy of

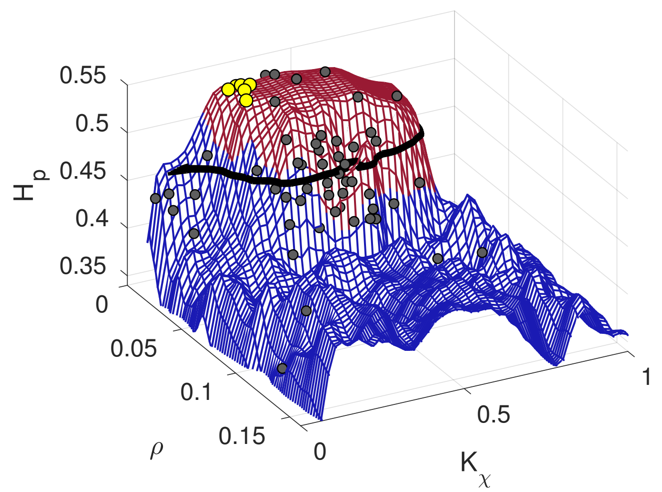

Fig. 5: Steering entropy H_p for fixed $K_M = 1.6$ and for varying ρ and K_χ. The surface region in red corresponds to stable parameter combinations while the blue region is unstable. The optima for low workload driving (Section IV-A) are displayed as yellow dots. In black, the contour line for $H_p \approx 0.47$ is shown. The gray dots are fitted values from NDD.

attentive drivers – not performing additional tasks such as attending a conversation or typing into a cell phone [10].

In Figure 5 the steering entropy is plotted for different control parameters. The magnitude of H_p was obtained by running the vehicle simulation with $K_M = 1.6$ – which approximately corresponds to the mean value found in the Pareto front – and with different values for ρ and K_χ. In the same figure, the contour line corresponding to $H_p = 0.47$ is displayed. The optimized values obtained in Section IV-A are also visible.

The optimized parameters produce higher values of H_p than those found in typical human drivers ($Hp \approx 0.54$). In particular, the optimal points present a steering entropy analogous to that of a partially distracted driver checking a navigation display – but certainly not due to the same mechanism.

Commonly, driver parameters vary during the course of the driving task [21]. With this in mind, sliced segments – lasting for 5 s – of the steering signal from NDD [7] were utilized to fit the parameters of the model (11). This was done by keeping K_M fixed – again to 1.6 – and fitting ρ and K_χ to minimize the mean squared error between the SWA of the human drivers and the model. The fitted parameters are shown in Fig. 5. Because human control is partially stochastic – as a result of variable response delays due to varying levels of attention – the fitted parameters appear scattered, but with higher density in the stable region near $H_p \approx 0.47$.

Taking this into account two different sets of parameters are now compared. In Case A, an *optimizing driver* – according to (8) – with parameters in the Pareto front $K_M = 1.6, \rho = 0.02$ and $K_\chi = 0.3$ is considered. Case B, represents a driver with parameters fitted from NDD: $K_M = 1.6$, $\rho = 0.05$ and $K_\chi = 0.48$. The simulation was run for Case A and Case B with the same pseudo-random perturbation, so the model was responding to the same input in both cases. As

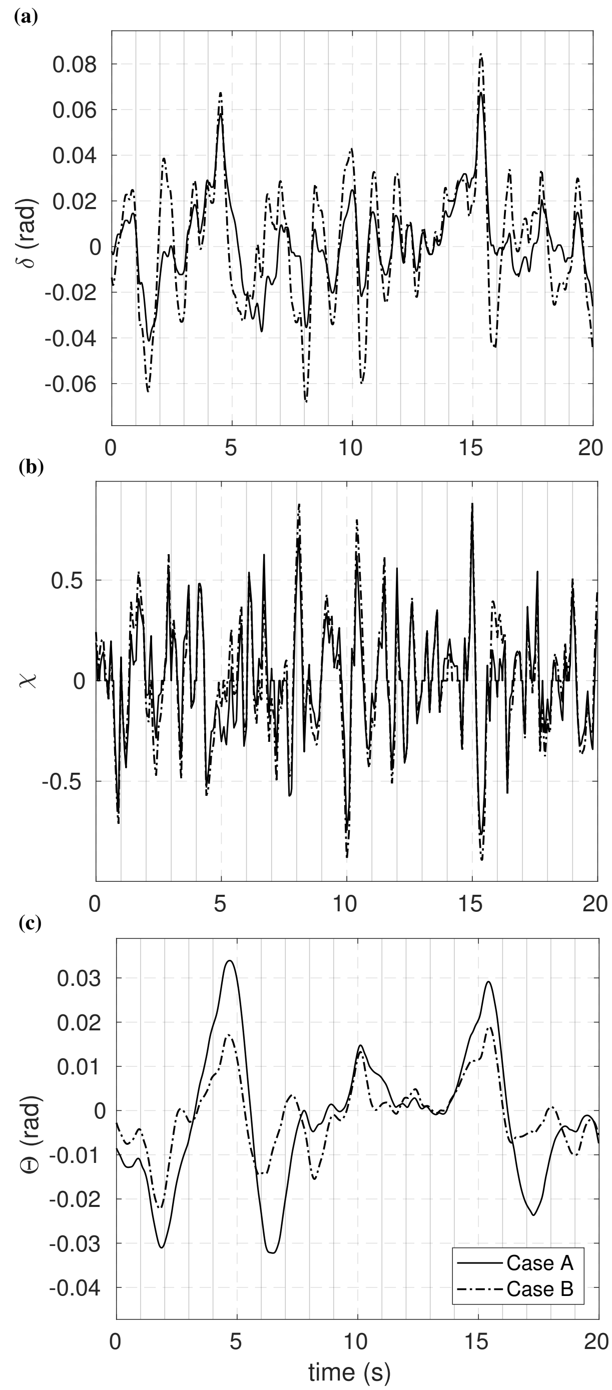

Fig. 6: (a) Response of the model (11), (b) CNYR (χ) and (c) splay error (Θ) for simulated data with two different sets of parameters: $\{K_M = 1.6, \rho = 0.02, K_\chi = 0.3\}$ (Case A) and $\{K_M = 1.6, \rho = 0.05, K_\chi = 0.48\}$ (Case B).

expected, for Case B the steering response has a higher gain and in some instants occurs earlier than in Case A (Fig. 6a). In both cases, the far-point error control is relatively similar, although with slightly higher amplitude peaks in Case B; this is due to the effect of the steering pulses of the MHC model (Fig. 6b). Further, Case B exhibits a significantly lower splay error Θ (Fig. 6c). And lastly, Case B yields a higher steering workload ($W_s = 0.39$) as compared to Case A ($W_s = 0.11$). Thus Case B reflects a *satisficing driver* according to W_s. The optimization process (Section IV-B) seems to have placed excessive emphasis on W_s minimization, due to the fact that small increments in ρ can place the model near instability.

V. Conclusions

In this paper, a new model of human steering control, based on far-point error perception and multiplicative control has been presented. The model was developed by considering different aspects of actual driver behavior.

In the first place, potential variables for steering control are identified: the *splay error* and the *critical normalized yaw rate*. These variables are consistent with neuroscience aspects of visual acquisition. The splay error is an optical variable as it is directly projected in the retina. It acts as a lane positioning variable for lane keeping. Nevertheless, although the splay error represents the near-region of the road, it can be identified by looking far ahead in the visual field. Further, it can be determined when only a part of the lane boundaries is visible. Thus it is a robust variable for human steering control and for computer vision systems as well. Part of the intended future work is directed towards determining how the critical normalized yaw rate can be characterized as an optical variable.

Low speed steering control was analyzed next. As multiplicative control reproduces the dynamical aspects of the human operator in compensatory tracking tasks, a multiplicative human control model was implemented to respond to the near region information of the road – the splay error. Interestingly, this model exhibits a response with characteristic *elementary steering pulses* similar to human steering control.

For higher speed driving an integral control law, based on the critical normalized yaw rate, was incorporated into the model. Accordingly, it has been shown that the model is stable with different sets of parameters, representing different driver states; variation of the parameters within their stable region exemplifies shifting levels of steering workload within the driving task. To conclude, the parameters fitted to match naturalistic driving data led to driver models that matched the steering entropy of attentive human drivers, unlike those obtained by performance optimization.

Appendix
Calculation of the Steering Entropy

The steering entropy (H_p) is obtained by first computing the difference between a steering signal $\delta(t_k)$ and its prediction $\tilde{\delta}(t_k)$. The prediction $\tilde{\delta}(t_k)$ results from the second order Taylor series approximation of $\delta(t)$ at every time step. From the prediction errors $e(t_k) = \delta(t_k) - \tilde{\delta}(t_k)$, the 90% percentile α is then calculated and the values $e(t)$ separated into the nine groups determined by the following bin edges: $\{-\infty, -5\alpha, -2.5\alpha, -\alpha, -1/2\alpha, 1/2\alpha, \alpha, 2.5\alpha, 5\alpha, \infty\}$. Lastly, the entropy of the percentage of values p_i ($i = 1, \ldots, 9$) inside each of the bins is obtained [10]:

$$H_p = -\sum_{i=1}^{9} p_i \log_9\{p_i\}. \tag{12}$$

References

[1] M. F. Land and D. N. Lee, "Where we look when we steer," *Nature*, vol. 369, no. 6483, pp. 742–744, 1994.

[2] M. Land and J. Horwood, "Which parts of the road guide steering?" *Nature*, vol. 377, no. 6547, pp. 339–340, 1995.

[3] R. L. Gregory, "Eye and brain: The psychology of seeing," 1997.

[4] R. Kodera, S. Tanahashi, A. Iijima, and Y. Maeda, "Measurement of eye movement in visual search for a target symbol and simulation to construct a small-world network," *Advanced Biomedical Engineering*, vol. 6, pp. 129–133, 2017.

[5] M. Kondo, "Directional stability (when steering is added)," *Journal of the Society of Automotive Engineers of Japan (JSAE)*, vol. 7, no. 5-6, p. 9, 1953.

[6] C. C. MacAdam, "Application of an optimal preview control for simulation of closed-loop automobile driving," *IEEE TRANSACTIONS ON SYSTEMS, MAN, AND CYBERNETICS*, 1981.

[7] M. Martinez-Garcia, Y. Zhang, and T. Gordon, "Modeling lane keeping by a hybrid open-closed-loop pulse control scheme," *IEEE Transactions on Industrial Informatics*, vol. 12, no. 6, pp. 2256–2265, 2016.

[8] M. Martínez-García and T. Gordon, "A multiplicative human steering control model," in *2017 IEEE International Conference on Systems, Man, and Cybernetics (SMC)*, Oct 2017, pp. 1–6.

[9] T. Gordon and K. Srinivasan, "Modeling human lane keeping control in highway driving with validation by naturalistic data," in *Systems, Man and Cybernetics (SMC), 2014 IEEE International Conference on*. IEEE, 2014, pp. 2507–2512.

[10] O. Nakayama, T. Futami, T. Nakamura, and E. R. Boer, "Development of a steering entropy method for evaluating driver workload," SAE Technical Paper, Tech. Rep., 1999.

[11] H. Guo, C. Shen, H. Zhang, H. Chen, and R. Jia, "Simultaneous trajectory planning and tracking using an mpc method for cyber-physical systems: A case study of obstacle avoidance for an intelligent vehicle," *IEEE Transactions on Industrial Informatics*, 2018.

[12] D. H. Hubel and T. N. Wiesel, "Receptive fields and functional architecture of monkey striate cortex," *The Journal of physiology*, vol. 195, no. 1, pp. 215–243, 1968.

[13] E. Yacoub, N. Harel, and K. Uğurbil, "High-field fmri unveils orientation columns in humans," *Proceedings of the National Academy of Sciences*, vol. 105, no. 30, pp. 10 607–10 612, 2008.

[14] D. D. Salvucci and R. Gray, "A two-point visual control model of steering," *Perception-London*, vol. 33, no. 10, pp. 1233–1248, 2004.

[15] E. Donges, "A two-level model of driver steering behavior," *Human Factors: The Journal of the Human Factors and Ergonomics Society*, vol. 20, no. 6, pp. 691–707, 1978.

[16] A. C. Beall and J. M. Loomis, "Visual control of steering without course information," *Perception*, vol. 25, no. 4, pp. 481–494, 1996.

[17] T. Gordon, A. Blankespoor, M. Barnes, D. Blower, P. Green, and L. Kostyniuk, "Yaw rate error–a dynamic measure of lane keeping control performance for the retrospective analysis of naturalistic driving data," in *21st International Technical Conference on the Enhanced Safety of Vehicles, Stuttgart, Germany*, 2009, pp. 09–0326.

[18] A. E. Bashirov, E. M. Kurpınar, and A. Özyapıcı, "Multiplicative calculus and its applications," *Journal of Mathematical Analysis and Applications*, vol. 337, no. 1, pp. 36–48, 2008.

[19] M. J. Wargo, "Human operator response speed, frequency, and flexibility: A review and analysis," *Human factors*, vol. 9, no. 3, pp. 221–238, 1967.

[20] IPG, "Carmaker®(5.0.1)," 2015-07-20, http://ipg.de/.

[21] J. Pauwelussen, "Dependencies of driver steering control parameters," *Vehicle system dynamics*, vol. 50, no. 6, pp. 939–959, 2012.

[22] K. J. Craik, "Theory of the human operator in control systems (i)," *British Journal of Psychology. General Section*, vol. 38, no. 2, pp. 56–61, 1947.

[23] ——, "Theory of the human operator in control systems (ii)," *British Journal of Psychology. General Section*, vol. 38, no. 3, pp. 142–148, 1948.

[24] W. Abend, E. Bizzi, and P. Morasso, "Human arm trajectory formation." *Brain: a journal of neurology*, vol. 105, no. Pt 2, pp. 331–348, 1982.

[25] O. Benderius and G. Markkula, "Evidence for a fundamental property of steering," in *Proceedings of the Human Factors and Ergonomics Society Annual Meeting*, vol. 58, no. 1. SAGE Publications, 2014, pp. 884–888.